Available online at www.sciencedirect.com
SCIENCE DIRECT
ELSEVIER
International Journal of Mass Spectrometry 254 (2006) 94–100
International Journal of Mass Spectrometry
www.elsevier.com/locate/ijms

Optimization of the conditions for simultaneous non-selective excitation of plutonium isotopes for isotope ratio measurements in resonance ionization mass spectrometry

M. Sankari, P.V. Kiran Kumar, M.V. Suryanarayana *

National Centre for Compositional Characterisation of Materials, Bhabha Atomic Research Centre, Department of Atomic Energy ECIL (PO), Hyderabad, Andhra Pradesh 500062, India

Received 24 April 2006; received in revised form 23 May 2006; accepted 24 May 2006

Abstract

Theoretical calculations based on density matrix formalism have been carried out for the non-selective excitation of the isotopes of plutonium for triple resonance excitation scheme with $\lambda_1 = 420.77$ nm, $\lambda_2 = 847.28$ nm and $\lambda_3 = 767.53$ nm. The effects of Doppler broadening, non-Lorentzian lineshape as well as time-dependent laser intensity profiles have all been incorporated. The threshold laser powers and bandwidths for the three excitation steps have been evaluated for non-selective excitation. The saturation behavior of the three excitation steps has been studied. The two-dimensional lineshape contour and its features have been investigated; while the reversal of peak asymmetry of two-step and two-photon excitation peaks under these conditions is discussed. The isotopic bias between the resonant and off-resonant isotope under the optimized conditions is observed to be not more than 3%. Application of RIMS under these conditions for isotope ratio measurements is outlined.

Keywords: Resonance ionization mass spectrometry; Isotope ratio; Pu; Laser spectroscopy; Mass spectrometry

1. Introduction

The knowledge of transuranium elements (TUE) is essential to determine their origin in the environment. Plutonium is the one of the most widespread elements among TUE and hence its isotopic composition is very important. Plutonium is released into the environment due to the fallout from nuclear weapons tests, various kinds of accidents as well as leakages from nuclear power plants and reprocessing facilities. The determination of the isotopic composition allows an assignment of the origin of the plutonium since each source shows a unique isotopic signature [1,2]. Therefore, determination of isotope ratios and concentration of plutonium at the ultra-trace level (fg/g) in environmental samples is important as it leads to the source of contamination and for safeguard purposes.

Normally, radiometric methods are used for the analysis of plutonium due to its simplicity and cost effective method of analysis, however these methods are not free from disadvantages. For example, α-spectroscopy of the long-lived isotopes ^{242}Pu and ^{244}Pu cannot be performed at ultra-trace levels. Furthermore, the energy resolution of most α-detectors is not good enough to distinguish between ^{239}Pu/^{240}Pu and ^{238}Pu/^{241}Am. ^{241}Pu which is a β-emitter, is not detectable by α-spectroscopy at all. Mass spectrometric methods are more suitable to obtain isotope ratio information as they are not dependent on the half-life or decay mode of the isotope. Among them thermal ionization mass spectrometry (TIMS) and inductively coupled plasma-mass spectrometer (ICP-MS) are most commonly used [3–6]. Recently, nano-volume flow injection double-focusing sector field inductively coupled plasma mass spectrometer (nFI-ICP-SFMS) has been used for the ultra-trace detection of ^{238}U and ^{242}Pu isotopes, wherein detection limits of 2.3×10^5 and 3.8×10^4 atoms have been reported, respectively [7]. However, isobaric interferences and peak tailing due to abundance sensitivity limit the potential of such techniques for the detection of ^{239}Pu isotope. Reduction of UH^+ formation has been reported using D_2O as solvent in ICP-SFMS thus eliminating isobaric interferences for the determination of ^{236}U/^{238}U isotope ratios [8]. Accelerator mass

* Corresponding author. Tel.: +91 40 27121365; fax: +91 40 27125463.
E-mail address: suryacccm@rediffmail.com (M.V. Suryanarayana).

1387-3806/$ – see front matter © 2006 Elsevier B.V. All rights reserved.
doi:10.1016/j.ijms.2006.05.019

spectrometry (AMS) has also been employed for the detection of Pu isotopes and isotope ratio measurements in the environmental samples [9]. The detection limits were reported as 1 fg (for ^{239}Pu). However, the prohibitively high cost of the equipment limits its widespread use. All methods described above require laborious sample preparation including matrix removal. Laser-ablation inductively coupled plasma mass spectrometry (LA–ICP-MS) was applied for direct analysis of Pu in soil and sediment samples with a modified laser-ablation system providing high ablation rates coupled with a sector-field ICP-MS resulting in detection limits as low as 300 fg for Pu isotopes in soil samples [10]. Except for sample inhomogeneity no other effects affecting measurement accuracy have been reported.

Resonance ionization mass spectrometry, on the other hand, has matured as a technique for ultra-trace detection and isotope ratio measurements [11–13]. However in this case, one has to carefully choose the excitation scheme, powers of the excitation lasers based on the analyte under consideration for efficient excitation and ionization. Recently, Grüning et al. [14] have used three-step excitation scheme for ultra-trace detection of Pu isotopes. They have achieved a detection limit of 2×10^6 atoms of Pu for single isotope measurements using high-repetition rate Nd:YAG pumped Ti:sapphire laser system, which allows efficient ionization of the resonant isotope. However, in order to carry out rapid isotope ratio measurement, it is necessary to ionize all the constituent plutonium isotopes efficiently and indiscriminately. Such condition cannot be achieved by arbitrary selection of the laser powers. However, by calculating the excitation lineshape for various excitation conditions, the optimum powers and bandwidth requirement of the excitation lasers for non-selective ionization of all the isotopes can be identified. The present work is motivated by the need to arrive at conditions for indiscriminate excitation/ionization of all the plutonium isotopes thereby facilitating isotope ratio measurements.

For the present investigations, we have chosen a three-step excitation scheme which has been employed earlier for ultra-trace analysis of plutonium [14]. The obvious advantage with the excitation scheme is that the wavelengths are accessible using the high-repetition rate solid state laser system which can be easily operated in a normal analytical laboratory. Effect of various parameters such as laser powers, detuning and bandwidth on the indiscriminate excitation of plutonium isotopes has been studied.

2. Theoretical description of the density matrix formalism for three-step excitation

In the three-step excitation scheme (Fig. 1), the plutonium isotopes from the [Rn] $5f^6\,7s^2$ ($^7F_0$) ground state are pumped into the first excited state [Rn] $5f^6\,7s\,7p$ ($^7D^0_1$) using the 420.77 nm laser light from a DPSS pumped frequency doubled Ti:sapphire laser. The atoms are then pumped into a higher level using the 847.26 nm laser light from another DPSS pumped Ti:sapphire laser. The atoms are then pumped into a high lying Rydberg level using the 767.53 nm laser light from the third DPSS pumped Ti:sapphire laser. These excited atoms are eventually ionized using an electric field.

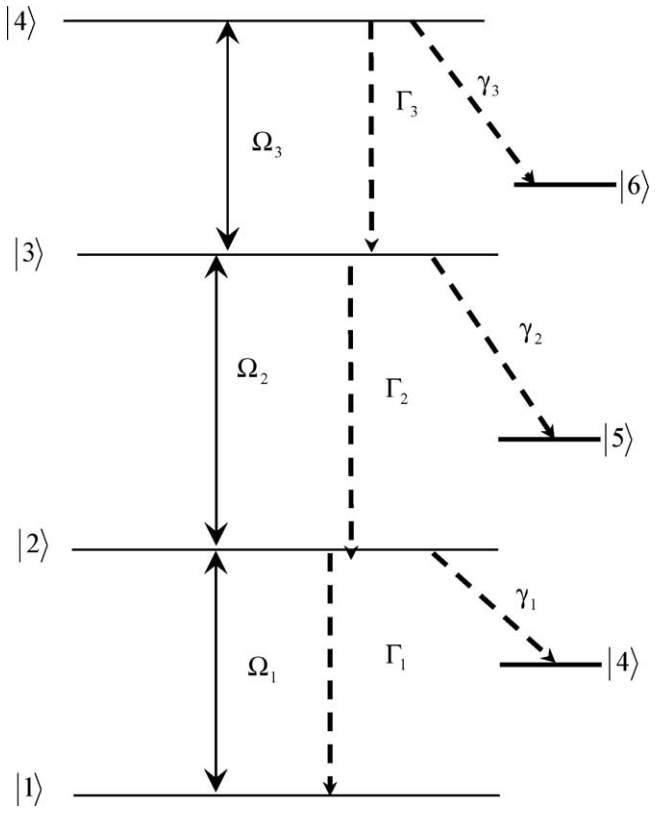

Fig. 1. Schematic of triple resonance scheme.

In a multi-step excitation process, the optical isotopic selectivity that can be achieved in a photo-excitation scheme is dependent on the isotope shifts in various excitation transitions, hyperfine structure, the dipole moments, the intensities of the excitation lasers and decay rates of the transitions [15–17]. Accurate and detailed description of the lineshapes obtained in multi-step resonance excitation processes with lasers cannot be predicted with a rate equation model, as it does not include the coherences established between the atomic states by the laser light fields.

Let $|1\rangle$, $|2\rangle$, $|3\rangle$ and $|4\rangle$ be the ground, first, second and third resonance states. Let $\hbar\omega_1$, $\hbar\omega_2$ and $\hbar\omega_3$ be the energies of the first, second and third resonance excitation transitions, respectively (Fig. 1). The three resonance excitation transitions are pumped by three different pulsed lasers having a phase diffusion bandwidth of a few GHz. The first, second and third excited states decay by a rate denoted by Γ_1, Γ_2 and Γ_3, respectively.

The electric fields of the lasers can be represented as:

$$E_i(t) = [\varepsilon_i(t)e^{i\omega_i t} + \varepsilon_i^*(t)e^{-i\omega_i t}]e_i \quad (1)$$

where e_i is the polarization vector and $\varepsilon_i(t)$ is the amplitude of the excitation laser. The interaction between the atom and laser field in the dipole approximation is given by $-\mu E(t)$ where μ is the dipole operator. The density matrix equations for the closed four-level atomic system for excitation into level $|4\rangle$ under the electric dipole and rotating wave approximation have been derived. The population dynamics in multi-step ladder excitation is described

by the following density matrix equations:

$$\dot{\rho}_{11} = \mathrm{i}(\Omega_1^*\rho_{21} - \Omega_1\rho_{12}) + 2\Gamma_1\rho_{22} \tag{2}$$

$$\dot{\rho}_{22} = \mathrm{i}(\Omega_1\rho_{12} - \Omega_1^*\rho_{21}) + \mathrm{i}(\Omega_2^*\rho_{32} - \Omega_2\rho_{23}) + 2\Gamma_2\rho_{33} - 2(\Gamma_1 + \gamma_1)\rho_{22} \tag{3}$$

$$\dot{\rho}_{12} = \mathrm{i}(\Delta_1\rho_{12} - \Omega_2\rho_{13}) + \mathrm{i}\Omega_1^*(\rho_{22} - \rho_{11}) - (\Gamma_1 + \gamma_1)\rho_{12} \tag{4}$$

$$\dot{\rho}_{21} = -\mathrm{i}(\Delta_1\rho_{21} - \Omega_2^*\rho_{31}) - \mathrm{i}\Omega_1(\rho_{22} - \rho_{11}) - (\Gamma_1 + \gamma_1)\rho_{21} \tag{5}$$

$$\dot{\rho}_{33} = \mathrm{i}\Omega_3^*\rho_{43} - \mathrm{i}\Omega_3\rho_{34} + \mathrm{i}(\Omega_2\rho_{23} - \Omega_2^*\rho_{32}) - 2(\Gamma_2 + \gamma_2)\rho_{33} + 2\Gamma_3\rho_{44} \tag{6}$$

$$\dot{\rho}_{13} = [\mathrm{i}(\Delta_1 + \Delta_2)\rho_{13} + \mathrm{i}\Omega_1^*\rho_{23} - \mathrm{i}\Omega_2^*\rho_{12} - \mathrm{i}\Omega_3\rho_{14}] - (\Gamma_2 + \gamma_2)\rho_{13} \tag{7}$$

$$\dot{\rho}_{31} = [-\mathrm{i}(\Delta_1 + \Delta_2)\rho_{31} - \mathrm{i}\Omega_1\rho_{32} + \mathrm{i}\Omega_2\rho_{21} + \mathrm{i}\Omega_3^*\rho_{41}] - (\Gamma_2 + \gamma_2)\rho_{31} \tag{8}$$

$$\dot{\rho}_{23} = [\mathrm{i}\Delta_2\rho_{23} + \mathrm{i}\Omega_1\rho_{13} - \mathrm{i}\Omega_3\rho_{24}] + \mathrm{i}\Omega_2^*(\rho_{33} - \rho_{22}) - (\Gamma_1 + \gamma_1 + \Gamma_2 + \gamma_2)\rho_{23} \tag{9}$$

$$\dot{\rho}_{32} = -[\mathrm{i}\Delta_2\rho_{32} + i\Omega_1^*\rho_{31} - i\Omega_3^*\rho_{42}] - i\Omega_2(\rho_{33} - \rho_{22}) - (\Gamma_1 + \gamma_1 + \Gamma_2 + \gamma_2)\rho_{32} \tag{10}$$

$$\dot{\rho}_{44} = \mathrm{i}(\Omega_3\rho_{34} - \Omega_3^*\rho_{43}) - 2(\Gamma_3 + \gamma_3)\rho_{44} \tag{11}$$

$$\dot{\rho}_{14} = [\mathrm{i}(\Delta_1 + \Delta_2 + \Delta_3)\rho_{14} + \mathrm{i}\Omega_1^*\rho_{24} - \mathrm{i}\Omega_3^*\rho_{13}] - (\Gamma_3 + \gamma_3)\rho_{14} \tag{12}$$

$$\dot{\rho}_{41} = [-\mathrm{i}(\Delta_1 + \Delta_2 + \Delta_3)\rho_{41} - \mathrm{i}\Omega_1\rho_{42} + \mathrm{i}\Omega_3\rho_{31}] - (\Gamma_3 + \gamma_3)\rho_{41} \tag{13}$$

$$\dot{\rho}_{24} = [\mathrm{i}(\Delta_2 + \Delta_3)\rho_{24} + \mathrm{i}\Omega_1\rho_{14} + \mathrm{i}\Omega_2^*\rho_{34} - \mathrm{i}\Omega_3^*\rho_{23}] - (\Gamma_1 + \gamma_1 + \Gamma_3 + \gamma_3)\rho_{24} \tag{14}$$

$$\dot{\rho}_{42} = [-\mathrm{i}(\Delta_2 + \Delta_3)\rho_{42} - \mathrm{i}\Omega_1^*\rho_{41} - \mathrm{i}\Omega_2\rho_{43} + \mathrm{i}\Omega_3\rho_{32}] - (\Gamma_1 + \gamma_1 + \Gamma_3 + \gamma_3)\rho_{42} \tag{15}$$

$$\dot{\rho}_{34} = [\mathrm{i}\Delta_3\rho_{34} + \mathrm{i}\Omega_2\rho_{24}] + \mathrm{i}(\Omega_3^*\rho_{44} - \Omega_3^*\rho_{33}) - (\Gamma_2 + \gamma_2 + \Gamma_3 + \gamma_3)\rho_{34} \tag{16}$$

$$\dot{\rho}_{43} = -[\mathrm{i}\Delta_3\rho_{43} + \mathrm{i}\Omega_2^*\rho_{42}] - \mathrm{i}(\Omega_3\rho_{44} - \Omega_3\rho_{33}) - (\Gamma_2 + \gamma_2 + \Gamma_3 + \gamma_3)\rho_{43} \tag{17}$$

ρ_{jk} represent the state population for $|j\rangle$ when $j = k$ and the coherence between states $|j\rangle$ and $|k\rangle$ when $j \neq k$. Ω_1, Ω_2 and Ω_3 are the Rabi frequencies of the first, second and third resonance excitation transitions, Δ_1, Δ_2 and Δ_3 are the rest frame detunings of the laser frequencies from the atomic resonance frequencies.

The Rabi frequencies of the three excitation steps can be evaluated from the transition dipole matrix elements $\langle a|\hat{r}|b\rangle$. The transition dipole matrix elements can be expressed in terms of spontaneous emission rate A_{nm}.

$$|\langle a|\hat{r}|b\rangle|^2 = 4.94 \times 10^{-16}\lambda^3 A_{\mathrm{nm}} \tag{18}$$

where λ is the transition wavelength in nm and A_{nm} is expressed in s^{-1}, while the dipole matrix element is in atomic units [18].

The effects of the laser spectral lineshape, which is assumed to arise from phase fluctuations, are included in the terms,

$$2\gamma_{\mathrm{L}}\frac{\beta_i^2}{\Delta_i^2 + \beta_i^2}, \quad i = 1, 2, 3 \tag{19}$$

In this phase diffusion model, the laser spectrum is Lorentzian near the center with full width at half maximum (FWHM) γ_{Li} ($i = 1, 2, 3$) and has a cutoff around β_i ($i = 1, 2, 3$) [19]. For detunings $\Delta_i \ll \beta_i$ ($i = 1, 2, 3$), these terms reduce to γ_{Li}, while for $\Delta_i \gg \beta_i$, the lasers appear to be monochromatic.

In realistic situations, an atom irradiated by a laser is usually found to be moving with respect to the frame in which the frequency of the laser radiation is measured. A group of such atoms, in thermal equilibrium have a velocity distribution described by the Boltzmann distribution. Thus, the velocity distribution parallel to the laser beam is of Gaussian distribution. An atom moving with velocity "v" in the direction of irradiation sees an additional detuning corresponding to $\Delta = v \times (\nu/c)$ to the first order in ν/c, where ν is the frequency of the laser radiation. The average population distribution is then given by an integral over the individual populations weighted by the Gaussian distribution. Thus,

$$P_j = \int W(v_x)\rho_{jj}, \quad \text{where } j = 1,\ 2,\ 3,\ 4 \tag{20}$$

$W(v_x)$ is the Doppler velocity distribution such that

$$W(v_x) = \frac{N_{\mathrm{o}}}{v_{\mathrm{o}}\sqrt{\pi}}\exp\left[-\left(\frac{v_x}{v_{\mathrm{o}}}\right)^2\right] \tag{21}$$

where N_{o} is the atomic density and v_{o} is equal to most probable velocity.

The numerical integration of the coupled differential equations for the three-step excitation scheme was carried out for Gaussian shaped temporal laser profiles with FWHM of ~70 ns. The three laser beams are considered to be co-propagating with no temporal delay between the laser pulses. The numerical integration was carried out using adaptive step size fourth order Runge–Kutta method.

In the present investigations, we consider the atomization temperature of plutonium as 1300 K. The corresponding Doppler broadening of ~1.1 GHz is chosen for all the calculations.

3. Results and discussion

Resonance ionization mass spectrometry has been used to exploit the inherent selectivity in the excitation process arising due to the isotope shifts and low bandwidth of lasers [20,21] to achieve an optical isotopic selectivity of $\sim 10^{10}$ for sensitive determination of rare ^{41}Ca isotope in the presence of large excess of the high abundant isotope. The selectivity is due to the finite bandwidth of the excitation lasers and the isotope shift between the constituent isotopes. In order to determine the isotope ratios by RIMS, this inherent selectivity of the photo-excitation process should be eliminated by indiscriminate excitation of all the constituent isotopes. Thus, the corresponding isotopic ratio is determined without much bias [22–24]. In the present case, approaching such an idealistic condition is by no means a simple task considering the large isotope shifts of the plutonium isotopes. The obvious choice for isotope ratio measurements would be to use a very broadband laser, so that the entire spectral width of all the isotopes is overlapped and all the isotopes could be excited. However, the appropriate bandwidth of the excitation lasers and powers is inherently dependent on the isotope shifts among the constituent isotopes. Realistically, one can only minimize the selectivity of the excitation scheme under certain specific conditions with respect to the bandwidth and powers of the excitation lasers. In principle, a priori arriving at such conditions that yield non-selective ionization of various isotopes is possible by calculating the excitation efficiency of the upper level by density matrix formalism.

The isotope shifts of the plutonium isotopes for the first and second excitation transitions are plotted in Fig. 2. From the Fig. 2, it can be visualized that the frequency positions of the isotopes lie very nearly along the two-photon line. The isotope lying farthest from the resonance frequency of ^{240}Pu is ^{238}Pu isotope. Therefore, for any given experimental conditions when the lasers are tuned to the resonance of ^{240}Pu isotope, excitation efficiency of ^{238}Pu is expected to be smaller than any other isotope of plutonium. Therefore, in order to achieve indiscriminate (non-selective) excitation of all the constituent isotopes, it may be adequate to compare the excitation efficiency of ^{238}Pu with the excitation efficiency of the resonant ^{240}Pu isotope. Grüning et al. [14] have experimentally investigated an efficient three-step excitation and ionization scheme for plutonium with $\lambda_1 = 420.7$ nm, $\lambda_2 = 847.28$ nm and $\lambda_3 = 767.53$ nm for isotope selective ultra-trace analysis of plutonium as well as isotope ratio measurements of plutonium isotopes. They have measured the isotope shifts for the long-lived plutonium isotopes and have also studied the saturation behavior for all the three excitation steps. The saturation powers for the scheme investigated were reported to be 2 mW, 30 mW and 400 mW, respectively.

The experimental set up of Grüning et al. [14] consisted of three Nd:YAG pumped titanium–sapphire laser systems with laser linewidth of about 4.2 GHz, 3 GHz and 3 GHz, respectively for the three excitation steps. Initially, we have investigated the excitation efficiency of the resonant ^{240}Pu and off-resonant ^{238}Pu isotopes for the experimental conditions reported by Grüning et al., considering powers of 1 mW, 17 mW and 600 mW, respectively for the three excitation steps.

The excitation efficiency of plutonium isotopes is plotted as a function of the second laser detuning from ^{240}Pu resonance (Fig. 3), while the first laser is set to the resonance of ^{240}Pu isotope. From the plot, we observe that the excitation efficiency of the off-resonant ^{238}Pu isotope ($\sim$0.01%) is significantly smaller compared to the excitation efficiency of the resonant ^{240}Pu isotope ($\sim$1.8%). This plot indicates that, under these experimental conditions, certain amount of selectivity is unavoidable and hence, indiscriminate excitation and ionization of all the isotopes of plutonium is not feasible. Therefore, the isotope ratios can only be determined by sequentially tuning the lasers to the resonance frequencies of the constituent isotopes.

The degree of excitation of the off-resonant isotope can be increased by the use of broadband lasers (spectral overlap) or by increasing the power of the excitation lasers (power broadening). When the power of the excitation laser is more than the saturation power, the spectral lineshape gets broadened which is known as power broadening. In order to ensure comparable exci-

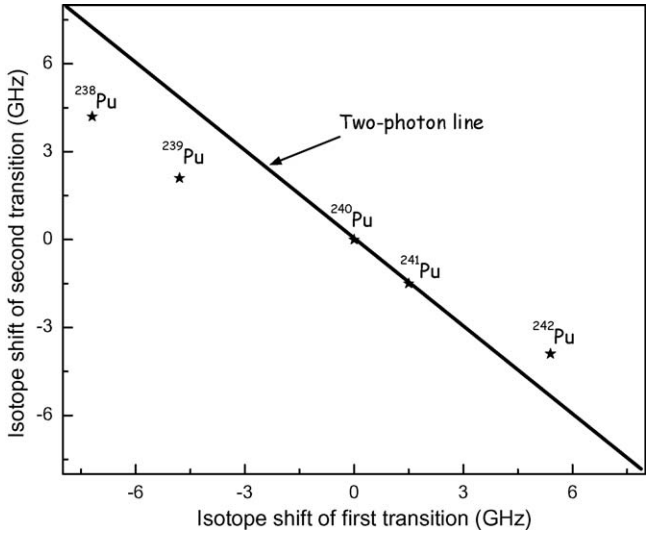

Fig. 2. Isotope shifts of various plutonium isotope relative to ^{240}Pu isotope for the first and second excitation transitions.

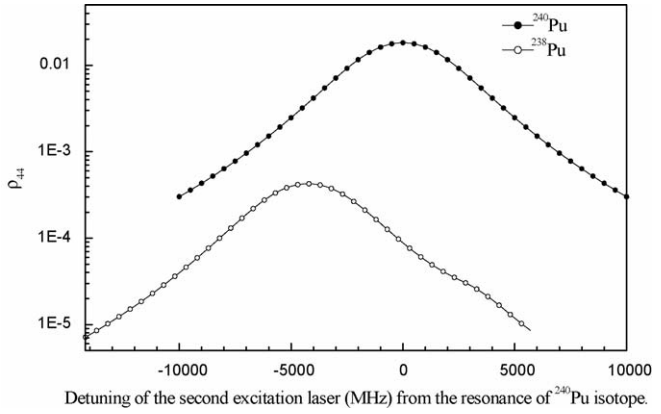

Fig. 3. One-dimensional lineshape of Pu isotopes. First excitation laser is tuned to the resonance of ^{240}Pu. The bandwidth of excitation lasers are 4.2 GHz, 3 GHz and 3 GHz for first, second and third excitation steps, respectively and the average powers are 1 mW, 17 mW and 600 mW at a repetition rate of 10 kHz.

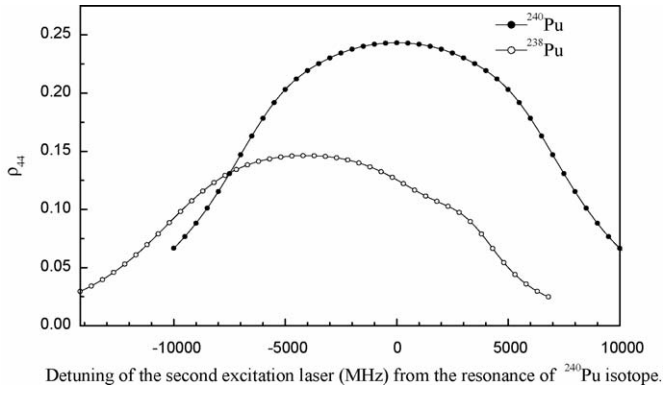

Fig. 4. One-dimensional lineshape of Pu isotopes. First excitation laser is tuned to the resonance of ^{240}Pu isotope. The bandwidth of excitation lasers are 4.2 GHz, 3 GHz and 3 GHz for the first, second and third excitation steps, respectively and the average powers are 544 mW, 248 mW and 1138 mW at a repetition rate of 10 kHz.

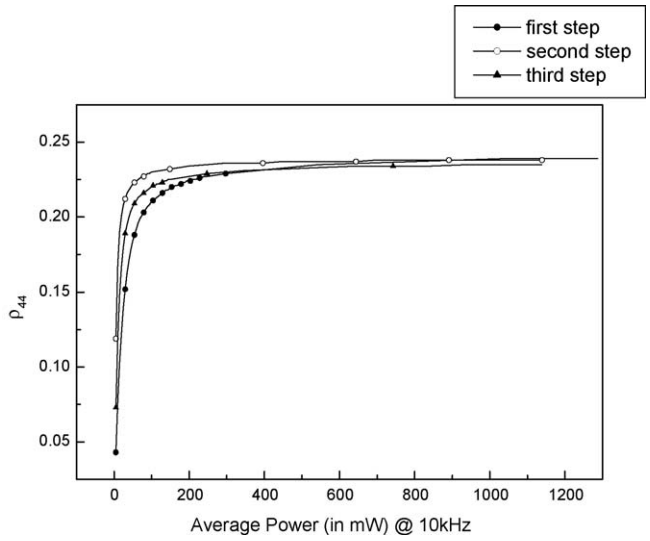

Fig. 5. Saturation behavior for the excitation steps for 10 GHz bandwidth lasers.

tation efficiency of the off-resonant ^{238}Pu isotope, the powers of the lasers must be sufficient to cause power broadening. Excitation efficiency of the resonant and off-resonant isotopes has been evaluated for various excitation powers to identify the conditions for non-selective excitation. We observe that ∼20% excitation efficiency is achievable for the resonant isotope even at very low powers of ∼50 mW for all the three excitation steps. However at these powers, the degree of excitation of the off-resonant ^{238}Pu isotope is about 0.4%; which is still far below for non-selective excitation. Excitation efficiency has been calculated by increasing the powers of all the three excitation lasers up to 2 W.

It was found that though the excitation efficiency of ∼24% for the resonant ^{240}Pu isotope is achievable, the excitation efficiency of the off-resonant ^{238}Pu isotope is only ∼13% (Fig. 4). Moreover, obtaining powers of ∼2 W for the first excitation laser is difficult due to the loss during frequency doubling. In spite of the appreciable increase in the laser powers, the excitation efficiency of the off-resonant isotope could not be increased beyond 13%. It may be worthwhile to note that even at very high excitation powers, the power broadening of the line profile is still insufficient to cause comparable degree of excitation of the off-resonant ^{238}Pu isotope with respect to the resonant ^{240}Pu isotope. Though this is not entirely unexpected; this result is primarily a manifestation of the large isotope shift of the first step. The bandwidth of the excitation laser is not adequate to cause appreciable amount of excitation of the off-resonant isotope (^{238}Pu) in comparison to the excitation efficiency of the resonant isotope (^{240}Pu). When the excitation lasers are tuned to ^{240}Pu isotope, the excitation efficiency of the off-resonant isotope is limited by the bandwidth of the excitation lasers rather than the powers. As mentioned earlier, under these bandwidth conditions indiscriminate excitation is not feasible even at large powers. Hence it can be concluded that a bandwidth of ∼3 GHz is insufficient and needs to be further increased.

Since the isotope shifts of ^{238}Pu are about −7.2 GHz and +4.2 GHz in the first and second excitation steps, respectively, a bandwidth > 7 GHz may be required for the complete overlap of the constituent isotopes. Therefore, the bandwidth of all the excitation lasers is set to be 10 GHz. Knowledge of the saturation behavior of the three excitation steps is very essential, in order to estimate the influence of changes of the laser power on the excitation efficiency of the resonant and the off-resonant isotope during analytical measurements. The saturation powers for the excitation steps have been evaluated, by calculating the excitation efficiencies for various average powers and are plotted in Fig. 5.

The limiting value of the degree of excitation efficiency to ∼25% is an indication that saturation condition has been reached and hence, any further increase in the laser powers shows only a marginal change in the excitation efficiency. Since, non-selective excitation for these bandwidth conditions is of interest, we have also evaluated the excitation efficiency of the off-resonant isotope for various powers. The optimum (threshold) powers are then identified as those which yield an excitation efficiency of ∼20% for the off-resonant ^{238}Pu isotope. The powers are found to be 0.54 W, 0.25 W and 1.14 W, respectively. The excitation efficiencies (Fig. 6) for the ^{238}Pu and ^{240}Pu isotopes are found to be 20% and 23%, respectively, while this difference of ∼3% should be acceptable for indiscriminate excitation. Even under these conditions, one has to carefully set the powers of the exci-

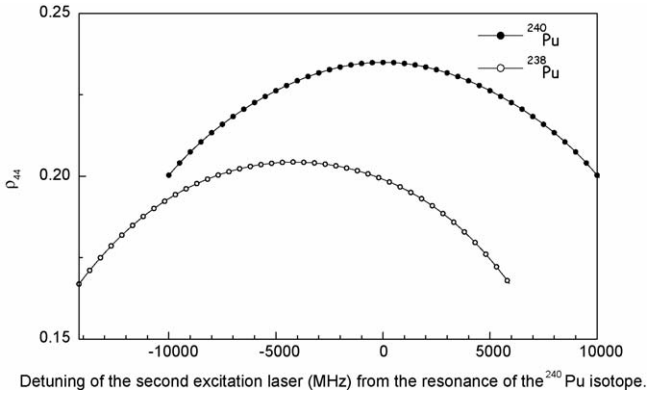

Fig. 6. One-dimensional lineshape of Pu isotopes. First excitation laser is tuned to the ^{240}Pu resonance. The bandwidth of excitation lasers are 10 GHz, 10 GHz and 10 GHz for first, second and third excitation steps, respectively and the average powers are 544 mW, 248 mW and 1138 mW at a repetition rate of 10 kHz.

tation lasers; else it may not lead to indiscriminate excitation. This can be illustrated by comparing the threshold conditions for achieving 20% excitation of the resonant isotope and the off-resonant isotope. Though an excitation efficiency of 20% for the resonant isotope is feasible at much smaller powers of 300 mW, 50 mW and 150 mW for the first, second and third steps, respectively, these values are not considered to be optimum since the degree of excitation of the off-resonant isotope is only 13%, leading to a significant bias in the excitation of the off-resonant isotope. With increase in the laser powers, the off-resonant isotope also falls into the power broadened width of the transition; thereby comparable excitation efficiencies are feasible for both the resonant and off-resonant isotopes. In summary, the calculations indicate that both the bandwidth and powers of the excitation lasers have significant role for indiscriminate and efficient excitation of all the isotopes.

The excitation efficiencies can be theoretically calculated by simultaneously detuning the first and the second excitation lasers from resonance, while keeping the third laser tuned to the resonance. Due to the smaller isotope shifts (<1 GHz) in the third excitation transition, it is adequate to plot two-dimensional contour of the excitation efficiency against the detuning of the first and the second excitation lasers (Fig. 7). A couple of interesting observations have been made. Firstly, the diagonal ridges along the line $\Delta\nu_1 + \Delta\nu_2 = 0$ which are the signature of coherent-two-photon excitation are totally absent. Secondly, the elliptical shape of the contour is a reflection of the magnitude of the power broadening along the two dimensions. The Rabi frequency of the second step is larger than that of the first step and hence the width along this dimension is larger than the width along the dimension of the first excitation laser. The perpendicular ridges in the dimension of $\Delta\nu_1 = 0$ MHz and $\Delta\nu_2 = 0$ MHz arising because of step-wise excitation ($|1\rangle \xrightarrow{\omega_1} |2\rangle \xrightarrow{\omega_2} |3\rangle$, are broadened leading to elliptical contours. The broadening of the perpendicular ridges along both the detuning axes clearly indicates a strong two-step excitation. This is because of the dominating power broadening in each excitation step and also the large bandwidth of the excitation lasers. As mentioned earlier, the isotopes of plutonium nearly fall along the diagonal two-photon ridge. The excitation efficiency along the diagonal two-photon line is nearly invariant up to the resonance frequency position of ^{238}Pu isotope which is a clear indication of the indiscriminate excitation of all the isotopes under these excitation conditions when the lasers are tuned to the resonance of ^{240}Pu isotope.

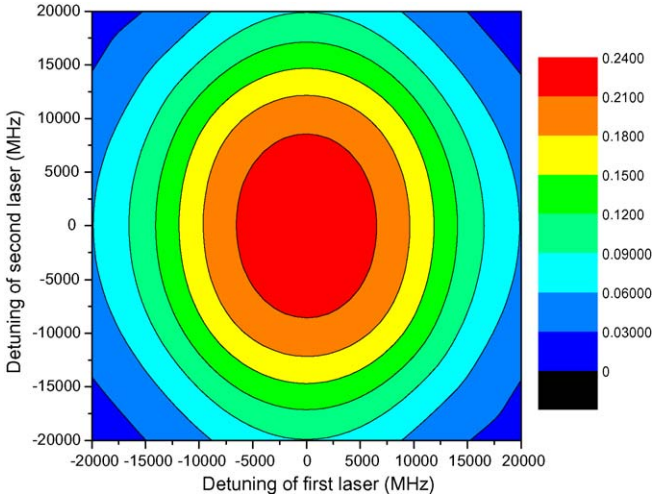

Fig. 7. Two-dimensional lineshape contour depicting the ρ_{44} for excitation lasers with bandwidth of 10 GHz.

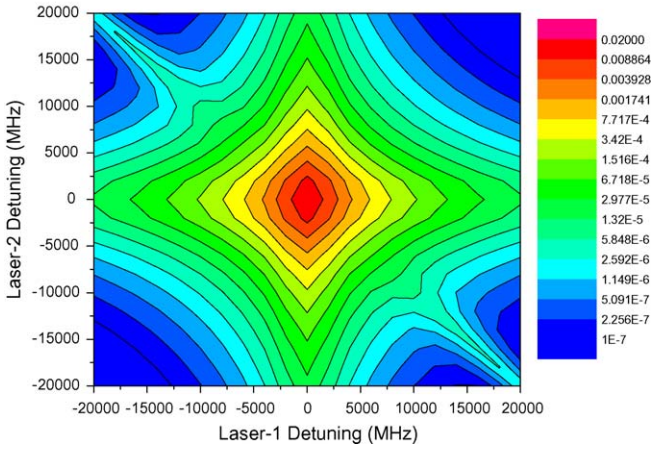

Fig. 8. Two-dimensional lineshape contour depicting the ρ_{44} for excitation lasers with bandwidth of 3 GHz and for the experimental conditions of Grüning et al. [14].

The two-dimensional lineshape for the experimental conditions reported by Grüning et al. [14] has also been plotted (Fig. 8). In this contour, the diagonal ridges arising due to the two-photon transition can be distinctly seen. Under these conditions, the perpendicular ridges due to step-wise excitation around $\Delta\nu_1 = 0$ MHz and $\Delta\nu_2 = 0$ MHz are dominating over the diagonal ridges. From the plot we observe reversal of asymmetry in the peaks heights, i.e., the two-photon excitation is weaker than the step-wise excitation. In general, when the excitation lasers are monochromatic, a normal asymmetry is observed wherein the two-photon peak dominates the two-step peak. Hence distinct diagonal ridge along the line $\Delta\nu_1 + \Delta\nu_2 = 0$ can be seen in the two-dimensional lineshape contour. Further, the relative strength of the coherent two-photon excitation peak and the step-wise excitation peak is a complex function of the Rabi frequencies (powers) of the two transitions, detuning and decay rates of the corresponding levels involved, the bandwidth of the excitation lasers and the Doppler broadening. Under the conditions reported by Grüning et al. [14], the reversal of asymmetry is observed which is solely attributed to the large bandwidth of the excitation lasers. The large bandwidth of the excitation lasers causes appreciable excitation due to wings of the laser profile even at detuned frequency conditions. As a result, reversal of asymmetry occurs. Under these conditions, the off-resonant isotopes which are along the two-photon excitation line are not excited appreciably, resulting in selective excitation. Therefore, isotope ratios can be determined by sequential excitation. At much higher bandwidths and powers (Fig. 7), two-photon peak merge with the step-wise excitation peak. Under these conditions, excitation can only be described by step-wise excitation resulting in the comparable excitation of the off-resonant iso-

topes too, thereby, enhancing the probability for simultaneous excitation of all plutonium isotopes.

4. Conclusions

The threshold powers and bandwidth of the excitation lasers required for indiscriminate excitation of all the isotopes of plutonium in a three-step resonance excitation scheme have been identified by using density matrix formalism. The saturation behavior of the three-excitation steps has been studied. Maximum excitation efficiency is found to be ∼23% for the resonant isotope. Under these optimized conditions, the isotopic bias between the resonant and the farthest lying off-resonant isotope can be utmost ∼3%. The optimized powers for the indiscriminate excitation of all the plutonium isotopes have been found to be 540 mW, 250 mW and 1138 mW for the first, second and third excitation steps, respectively, while the bandwidth requirement of the excitation lasers is ∼10 GHz. However, for the case of odd isotopes, the excitation efficiency has a preferential bias over the even isotopes due to its hyperfine structure. Hence, the excitation efficiency of the odd isotopes is expected to be comparable or higher than the resonant ^{240}Pu isotope. The present conditions for simultaneous isotope ratio determination result in a bias of ∼3% between the resonant and off-resonant isotope. However, the true isotope ratios can be retrieved by evaluating the bias using standard reference materials. Finally, the optimized parameters are expected to be useful for the rapid determination of plutonium isotope ratios for safeguard applications. An experimental facility is being planned based on these optimized powers and linewidths for the determination of isotopic composition and quantification of plutonium isotopes in environmental samples.

References

[1] M. Magara, Y. Hanzawa, F. Esaka, Y. Miyamoto, K. Yasuda, K. Watanabe, S. Usuda, H. Nishimura, T. Adachi, Appl. Radiat. Isotopes 53 (2000) 87.
[2] M. Nunnemann, N. Erdmann, H.-U. Hasse, G. Huber, J.V. Kratz, P. Kunz, A. Mansel, G. Passlera, O. Stetzer, N. Trautmann, A. Waldek, J. Alloys Compd. 271–273 (1998) 45.
[3] S.F. Boulyga, C. Testa, D. Desideri, J.S. Becker, J. Anal. Atom. Spectrom. 16 (2001) 1283.
[4] S.F. Boulyga, J.S. Becker, J. Anal. Atom. Spectrom. 17 (2002) 1143.
[5] S.F. Boulyga, J.L. Matusevich, V.P. Mironov, V.P. Kudrjashov, L. Halicz, I. Segal, J.A. McLean, A. Montaser, J.S. Becker, J. Anal. Atom. Spectrom. 17 (2002) 958.
[6] J.S. Becker, M. Zoriy, L. Halicz, N. Teplyakov, Chr. Muller, I. Segal, C. Pickhardt, I.T. Platzner, J. Anal. Atom. Spectrom. 19 (2004) 1257.
[7] D. Schaumloffel, P. Giusti, M.V. Zoriy, C. Pickhardt, J. Szpunar, R. Lobinski, J.S. Becker, J. Anal. Atom. Spectrom. 20 (2005) 17.
[8] M.V. Zoriy, L. Halicz, M.E. Ketterer, C. Pickhardt, P. Ostapczuk, J.S. Becker, J. Anal. Atom. Spectrom. 19 (2004) 362.
[9] D.H. Oughton, L. Skipperud, L.K. Fifield, R.G. Cresswell, B. Salbu, P. Day, Appl. Radiat. Isotopes 61 (2004) 249.
[10] S.F. Boulyga, M. Tibi, K.G. Heumann, Anal. Bioanal. Chem. 378 (2004) 342.
[11] K. Wendt, K. Blaum, B.A. Bushaw, C. Grunning, R. Horn, G. Huber, J.V. Kratz, P. Kunz, P. Muller, W. Nortershauser, M. Nunnemann, G. Passler, A. Schmitt, N. Trautmann, A. Waldek, Fresenius J. Anal. Chem. 364 (1999) 471.
[12] N. Erdmann, M. Nunnemann, K. Eberhardt, G. Hermann, G. Huber, S. Kohler, J.V. Kratz, G. Passler, J.R. Peterson, N. Trautmann, A. Waldek, J. Alloys Compd. 271 (1998) 837.
[13] P. Kunz, G. Huber, G. Passler, N. Trautmann, Eur. Phys. J. D 29 (2004) 183.
[14] C. Grüning, G. Huber, P. Klopp, J.V. Kratz, P. Kunz, G. Passler, N. Trautmann, A. Waldek, K. Wendt, Int. J. Mass Spectrom. 235 (2004) 171.
[15] M. Sankari, P.V. Kiran Kumar, M.V. Suryanarayana, J. Opt. Soc. Am. 21B (2004) 1369.
[16] P.V. Kiran Kumar, M.V. Suryanarayana, S. Gangadharan, J. Nuclear Mater. 282 (2000) 255.
[17] M. Sankari, P.V. Kiran Kumar, M.V. Suryanarayana, J. Phys. B: At. Mol. Opt. Phys. 33 (2000) 4927.
[18] B.S. Brandsden, C.J. Joachain, Physics of Atoms and Molecules, Longman Group Ltd., Harlow, 1983.
[19] P. Zoller, P. Lambropoulos, J. Phys. 12B (1979) L547.
[20] B.A. Bushaw, W. Nortershauser, K. Wendt, Spectrochim. Acta 54B (1999) 321.
[21] W. Nortershauser, B.A. Bushaw, P. Muller, K. Wendt, Appl. Opt. 39 (2000) 5590.
[22] M.G. Payne, S.L. Allman, J.E. Parks, Spectrochim. Acta 46B (1991) 1439.
[23] W.D. Brandon, W.R. Garrett, C.H. Chen, S.L. Allman, M.G. Payne, Spectrochim. Acta 49B (1994) 1057.
[24] W.M. Fairbank Jr., M.T. Spaar, J.E. Parks, J.M.R. Hutchinson, Phys. Rev. 40A (1989) 2195.